2003-01-1249

On the application of numerical methods for the calculation of the external aerodynamics of a streamlined car body

Lopes, A.M.G
Departamento de Engenharia Mecânica, Universidade de Coimbra, Portugal

Carvalheira, P.
Departamento de Engenharia Mecânica, Universidade de Coimbra, Portugal

ABSTRACT

The present paper describes the application of a numerical tool for the evaluation of the aerodynamic performance of a streamlined car shape. The numerical simulations are carried out using a commercial code based on an unstructured grid layout. Tests are made using the k-ε turbulence model and the Shear Stress Transport model. The influence of the advection scheme is also studied. The experimental measurements are made on a Gottingen-type wind tunnel with a test section of 2x2x8 m^3. Computations are compared with experimental values for the surface pressure distribution and measured forces.

INTRODUCTION

Numerical simulation is becoming a tool of growing importance in the field of fluid dynamics. The role of experimental measurement does not tend to be replaced by the numerical approach, due to inherent advantages that the actual measurement possesses. Nevertheless, in what concerns aerodynamic design and testing, at least, wind tunnel experimentation is a very expensive and time-consuming process. This applies for both the construction of the models and the measurement process. The numerical approach is not affected by these disadvantages. Changing the shape of a model and evaluating the new aerodynamic performance with a new computer run is a much more simple process than if a new model was to be built and tested in the wind tunnel. Furthermore, the enormous improvement in computer performance both in terms of speed and memory capacity, together with the decreasing of computer hardware price renders numerical simulation an attractive alternative to the wind tunnel approach. Numerical methods possess, nevertheless, limitations that are still not resolved. Turbulence modeling is a developing area of research, as no model is yet available for accurate predictions over a wide range of fluid flow situations. In what concerns automotive vehicles, the airflow pattern is, in the large majority of cases, characterized by separation. This leads to poorer accuracy in drag prediction. Errors in the range of 10 % to 20 % are common, and these are very much dependent on the type of geometry, as may be concluded from several works published in the literature for aerodynamic simulations around passenger cars (e.g. Kataoka *et al.*, 1991; Himeno *et al.*, 1990; Okumura and Kuriyama, 1995; Kawaguchi. *et al.*, 1989; Han *et al.*, 1996). Most of these works rely on the high-*Re* k-ε turbulence model (Launder and Spalding, 1974). Basara *et al.* (2001) point out the advantage of the Reynolds Stress model over the standard k-ε model, when simulating the flow for a Peugeot 405, a SAE body and a WC-CFD body. Ramnefors *et al.* (1996) report on mesh and turbulence model errors for the case of a Volvo Environmental Concept Car. These authors stress how a proper converged solution, along with double precision solver are necessary to ensure proper solution convergence with a second-order behaviour, as dependence on mesh refinement. These authors, nevertheless, do not test the grid surface clustering influence on the computed aerodynamic coefficients.

Prediction errors are very much dependent on the flow characteristics, and thus, on the car geometry. Flows with separation are, in principle, more difficult to model than attached flows. The present work deals with a streamlined car body shape where most of the drag occurs due to the surface shear stress. The aim of this work is to assess the applicability of numerical models to the prediction of the drag coefficient for a car prototype. The geometry pertains a three-wheel vehicle, which was built to an European consumption contest. Numerical simulations were carried out using the commercial package CFX 5.5, developed by AEA Technology. This code works on an unstructured mesh, and provides different approaches in terms of turbulence modeling. Grid and turbulence model dependence tests are shown and comparisons against experimental data are presented.

THE NUMERICAL MODEL

CFX 5.5 employs an unstructured grid, which is a major contribution for numerical robustness and geometric flexibility. Amongst the different turbulence models available, the standard k-ε model and the SST (Shear Stress Transport) model were selected for testing. For studying the influence of the advection scheme, the upwind and a higher-order discretization scheme were employed.

GRID GENERATION

The unstructured grid of CFX 5.5 is based on triangular element discretization for the generation of surface grids. The volume grid is constituted by tetrahedral elements, produced through the Advancing Font and Inflation method (*c.f.* CFX documentation for details). Near the surfaces, an inflation layer may be optionally produced, in order to better resolve boundary gradients. This inflation layer is made of prismatic and pyramidal elements. Global length, surface maximum and minimum length and inflation are some of the grid control parameters used in the grid generation module of CFX 5.5. They control, respectively, the grid size inside the domain, far from the boundaries; the maximum and minimum allowed grid size in the surface; and the thickness of the prismatic elements layer near the surface.

. THE k-ε TURBULENCE MODEL

The k-ε model available in CFX 5.5 is a standard high Reynolds (Launder and Spalding, 1974). CFX implements scalable wall functions that remove the problem of inconsistency of the wall function method in the case of fine grids. The basic idea is to assume that the surface coincides with the edge of the viscous sub-layer, defined as the intersection of the logarithmic and the linear near wall profile. Thus, the computed y^+ is not allowed to fall below this limit and all the grid points will be outside the viscous sub-layer (*c.f.* Vieser, 2002, for details).

THE SST TURBULENCE MODEL

The SST model was proposed by Menter (1993, 1994). It is a blend of the k-ω model (Wilcox, 1993), and the standard k-ε of Launder and Spalding (1974), according to the boundary layer region where the solution takes place. The equations are:

$$\frac{\partial}{\partial x_i}(\rho u_i k) = \frac{\partial}{\partial x_i}\left[\left(\mu + \frac{\mu_t}{\sigma_{k3}}\right)\frac{\partial k}{\partial x_i}\right] + P_k - \beta' \rho k\omega \qquad (1)$$

$$\frac{\partial}{\partial x_i}(\rho u_i \omega) = \frac{\partial}{\partial x_i}\left[\left(\mu + \frac{\mu_t}{\sigma_{\omega 3}}\right)\frac{\partial \omega}{\partial x_i}\right] + \alpha_3 \frac{\omega}{k} P_k - \beta_3 \rho\omega^2 + (1 - F_1) 2\rho\sigma_{\omega 2} \frac{1}{\omega} \nabla k \nabla \omega \qquad (2)$$

where the index 3 coefficients are obtained as a linear combination of the index 1 (corresponding to the k-ε model) and the index 2 (corresponding to the k-ω model) coefficients, as defined next:

$$\beta' = 0.09 \qquad \alpha_1 = 5/9 \qquad \beta_1 = 3/40$$

$$\sigma_{k1} = 2 \qquad \sigma_{\omega 1} = 2 \qquad \alpha_2 = 0.44 \qquad (3)$$

$$\beta_2 = 0.0828 \qquad \sigma_{k2} = 1 \qquad \sigma_{\omega 2} = 0.856$$

As a means of limiting the turbulence kinetic energy production in stagnation regions, its term is computed as follows:

$$\widetilde{P}_k = min(P_k, 10\varepsilon) \qquad (4)$$

The weighting factor F_1 is obtained with the following equation:

$$F_1 = tanh\left(min\left(max\left(\frac{\sqrt{k}}{\beta' \omega y}, \frac{500\nu}{y^2 \omega} \right), \frac{4\rho\sigma_{\omega 2} k}{CD_{k\omega} y^2} \right)\right)^4 \qquad (5)$$

$$CD_{k\omega} = max\left(2\rho\sigma_{\omega 2} \frac{1}{\omega} \nabla k \nabla \omega, 1e-10 \right) \qquad (6)$$

The modelization of the shear stress transport is accomplished with a limiting factor in the formulation of the turbulence viscosity:

$$\upsilon_t = \frac{a_1 k}{max(a_1 \omega, SF_2)} \qquad (7)$$

where:

$$F_2 = tanh\left(max\left(\frac{2\sqrt{k}}{\beta' \omega y}, \frac{500\nu}{y^2 \omega} \right)\right)^2 \qquad (8)$$

and S quantifies the fluid deformation rate (*cf.* Menter 1993, 1994 and Vieser, 2002 for details).

SOME DEFINITIONS

This work will present the values for drag and lift coefficients. Total drag coefficient is computed as the sum of pressure and friction contributions:

$$C_D = C_{D_f} + C_{D_p} = \frac{D_f + D_p}{0.5\rho U_{ref}^2 A_f} \quad (9)$$

where U_{ref} is the incoming free stream velocity and A_f is the vehicle frontal area. Each drag is obtained by adding the contributions from each control volume lying on the car surface, projected along the streamwise direction:

$$D_f = \sum\left(\mu A_f \frac{U_1}{\delta}\right)_x \quad D_p = \sum\left(-PA_f\right)_x \quad (10)$$

were δ is the distance to the surface, U_1 is the wind velocity at the closest node to the surface, μ is the effective viscosity and the coordinate x is parallel to the streamwise direction. The lift coefficient, C_L, is defined in a similar way, for the forces along the vertical (z) direction. Pressure and shear stress coefficients are defined as follows:

$$C_f = \frac{\tau_w}{0.5\rho U_{ref}^2} \quad (11)$$

$$C_p = \frac{P - P_0}{0.5\rho U_{ref}^2} \quad (12)$$

where τ_w and P_0 are the wall shear stress and the reference pressure, respectively.

EXPERIMENTAL TESTS

The original car is 2.650 m length, 0.690 m wide and 0.650 m high. The frontal area is 0.346 m^2 and the surface area is 4.10 m^2. For the experimental tests, a 1:2.5 scale model, without wheels, was built and instrumented with 191 pressure taps (Figure 1). Surface pressure distribution and drag force were measured in a Gottingen type wind tunnel, with an exit nozzle of 2x2 m^2 and an open test section 8 m long. The boundary layer thickness is 5 cm, for an incident free stream wind speed of 10 m/s. For measuring the drag force, the car was hanged from the wind tunnel ceiling with thin steel strings (Figure 2) and a load cell was connected to the car trailing edge. For measuring the aerodynamic force exerted on the hanging wires, a shelter with the car shape was built and attached to the ground. The drag force measured using this arrangement was then used for correcting the total force, thus allowing the determination of the aerodynamic force on the car itself.

Figure 1 - Model at 1:2.5 scale instrumented with surface pressure taps.

Experimental surface pressure distribution and dependence of C_D on the Re number will be presented later on this report, along with the numerical results.

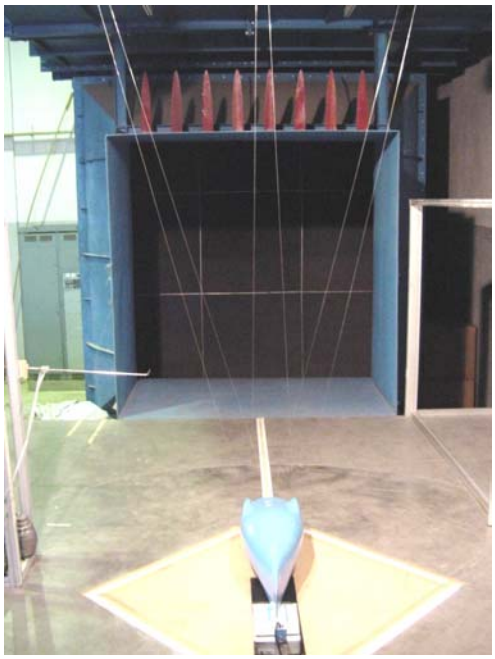

Figure 2 - Model in the wind tunnel

NUMERICAL SIMULATIONS

Grid topology and domain

The simulation domain is parallelepipedic, as depicted in Figure 3. As previously referred, the unstructured grid is composed by tetrahedral elements, with a prismatic layer near the surfaces. Figure 4 presents some selected grid planes for visualization.

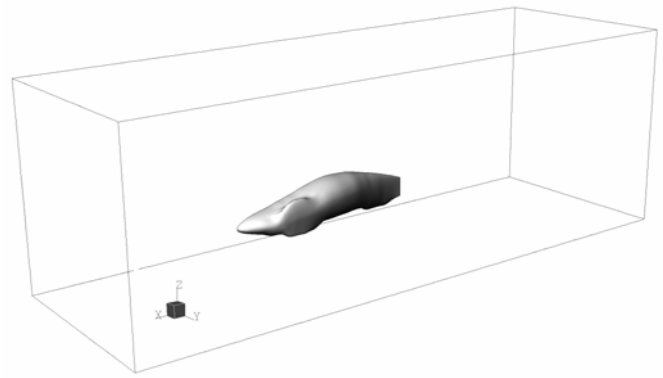

Figure 3 - Simulation domain.

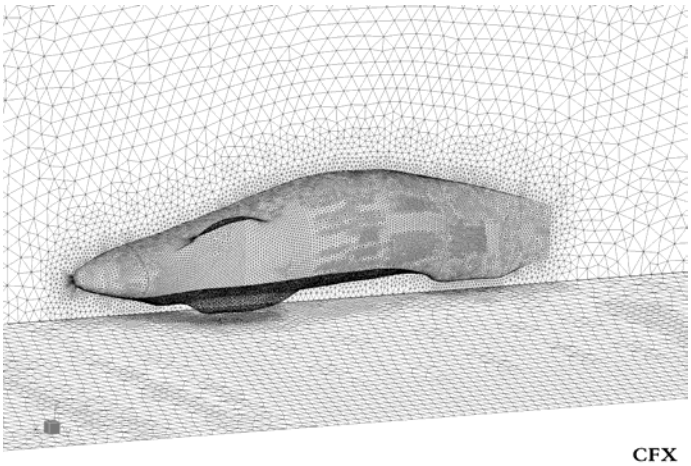

Figure 4 - Grid arrangement.

Boundary conditions and computer runs

Two types of simulations were carried out:

For grid dependence tests and C_D determination, a uniform incident velocity of 10 m/s with a turbulence intensity of 1% was set, and a non-slip wall moving at the same speed was set as boundary condition for the ground. This corresponds to "road conditions".

For comparison with wind tunnel measurements, a boundary-layer incident profile was considered in the simulations, with a turbulence intensity of 10 %. For reproducing wind tunnel conditions, the ground was considered as a stationary non-slip wall. Outer boundaries are free-slip walls.

Grid, turbulence models and differencing scheme tests

Grid tests were carried out changing both the grid size and grid clustering near the car surface (y+ values). Results were computed using the SST and k-ε turbulence models with the second-order differencing scheme. The corresponding data for SST model is listed in Table 1. Surface grid clustering is expressed via the y^+ value at the nodes closest to the car surface. Grids A to D were generated using similar surface clustering, changing the number of nodes on the car surface, and, consequently, the grid size in the vicinity of the car. Grids D0 to D4 correspond to different surface clustering distances. Analysis of these data reveals that the number of surface grid points influences mainly the drag pressure component, while the surface clustering (y^+ values) reflect mainly on the friction component of C_D. C_L values are much less affected by grid characteristics than C_D. Figures 5(a) and 5(b) display some of these data graphically. One may observe the asymptotical convergence of the computed C_D values with the total grid number of nodes, in Figure 5(a), where the horizontal line is the extrapolated value for C_D, using the Richardson extrapolation method. According to this method, a simulation will yield a quantity f that can be expressed in a general form by a Taylor expansion series:

$$f = f_{h=0} + g_1 h + g_2 h^2 + \ldots \quad (13)$$

where h is a representative grid spacing and the g coefficients are grid independent. If a second-order solution is obtained, then, neglecting higher order terms, the asymptotic solution (continuum value) may be obtained as follows:

$$f_{h=0} \cong f_1 + \frac{f_1 - f_2}{r^2 - 1} \quad (14)$$

where f_1 and f_2 are the solutions obtained in two different grids, and r is the grid ratio:

$$r = \frac{h_2}{h_1} \quad (15)$$

with h_1 smaller than h_2. The Richardson extrapolation yields C_D=*0.0735*, for both turbulence models.

It is interesting to note how much the C_D values are affected by surface clustering distance. CFX simulations yield an increase on C_D values with decreasing y^+, showing no asymptotic behaviour as y^+ tends to zero. A similar behaviour for both turbulence models is presented by Vieser *et al.* (2002), although with much lower variations. Extrapolation of these values using a quadratic function results in a C_D of 0.0883 for the k-ε model and a value of 0.0918 for the SST model (horizontal lines in graph b). Correcting for grid size, with the factor obtained from the Richardson extrapolation, values of 0.087 and 0.090 are obtained for the k-ε and the SST models, respectively. As may be seen later, a better agreement with the experimental C_D values is obtained neglecting the increase of C_D with y^+<2. This led us to question the validity of the simulations with such low y^+ values.

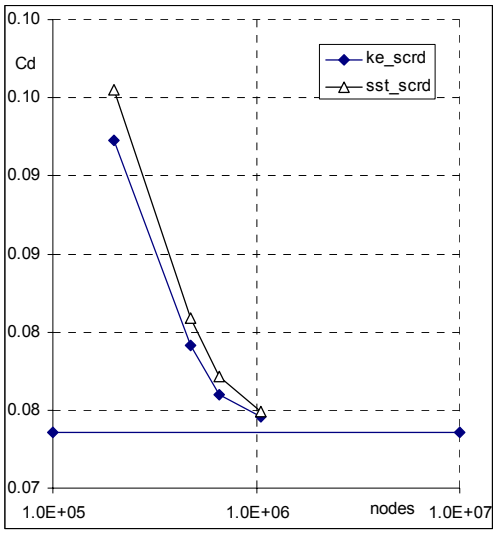

(a) - influence of total number of nodes

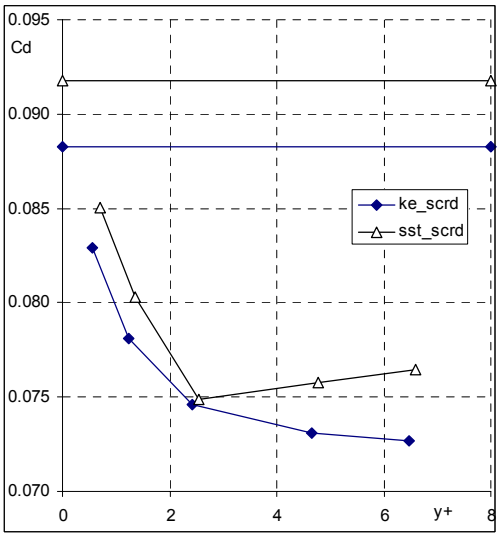

(b) - influence of surface clustering

Figure 5 **-** Effect of grid refinement on C_D.. Richardson extrapolation value in (a) is for both turbulence models.

Along with the SST model, the upwind and a second-order discretization scheme for the advection terms were tested. The results presented here are for Grid D. Table 2 summarizes the data thus obtained. It is interesting to note the role that the differencing scheme plays on the computed C_D. The first-order upwind scheme leads to C_D values much higher that the measured one. Analysis of CFX data shows that the differencing scheme affects mainly the pressure component of C_D. Stagnation pressure at the nose is quite close to the theoretical value of 1, for all the run cases.

Grid	nodes	y^+	C_{Dp}	C_{Df}	C_D	C_L
A	*198560*	2.67	0.0418	0.0511	0.0929	-0.2457
B	*472624*	2.58	0.0307	0.0502	0.0809	-0.2391
C	*657931*	2.59	0.0272	0.0500	0.0772	-0.2358
D	*1047534*	2.55	0.0266	0.0483	0.0749	-0.2375
D0	980638	*0.95*	0.0268	0.0582	0.0851	-0.2339
D1	980987	*1.35*	0.0266	0.0537	0.0803	-0.2342
D2	1047534	*2.55*	0.0266	0.0483	0.0749	-0.2375
D3	979000	*4.77*	0.0275	0.0483	0.0758	-0.2413
D4	978010	*6.60*	0.027	0.049	0.076	-0.244
Exp		-	-	-	0.0998	-

Table 1 **-** Grid dependence tests (SST_scrd). (*in italic: changing quantity*)

Table 2 **-** Turbulence and differencing scheme dependence. (results computed on Grid D)

	C_{Dp}	C_{Df}	C_D	C_L	$C_{p,nose}$
SST, secorder	0.0266	0.0483	0.0749	-0.2375	0.985
kε -secorder	0.0232	0.0514	0.0746	-0.2360	1.003
SST-upwind	0.1320	0.0609	0.1929	-0.3290	1.015
kε-upwind	0.1313	0.0640	0.1953	-0.3313	1.030
Exper.	-	-	0.0998	-	1.000

Subsequent results were all obtained using grid D. Figures 6 show the C_p variation along the car centerline. For the SST model, Figure 6(a) shows that the upwind scheme predicts higher pressure values upstream and lower pressure recovery downstream, leading to higher drag. Figure 6(b) shows that almost no differences exist between both turbulence models.

Figures 7 represent the shear stress coefficient on the top centerline of the car. As expected from previous results, the first-order scheme leads to higher values of the surface shear stress. It was found that the SST model presents rather high spatial fluctuations, as shown in (b). These fluctuations correspond to the grid spatial scale and are still to be completely explained. Computed C_D data with the lowest values of y^+ may have been affected by this behaviour.

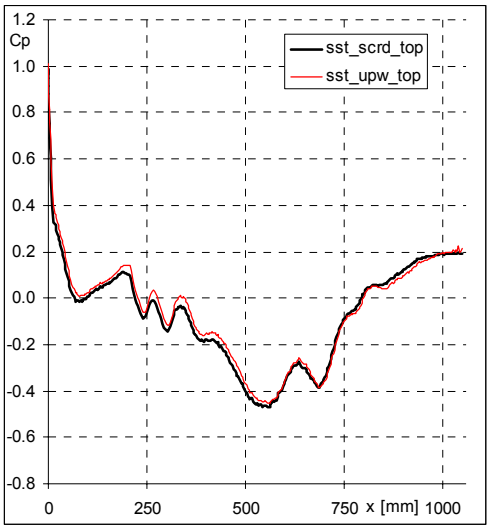

(a)

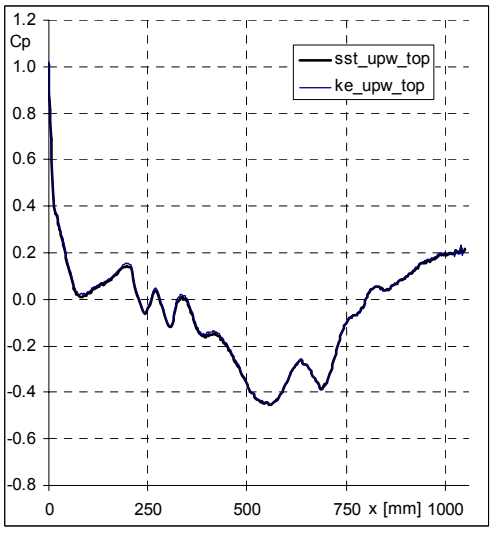

(b)

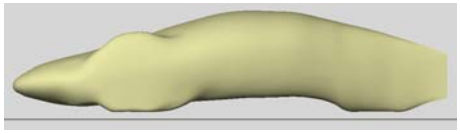

(a) - differencing scheme influence (b) - turbulence model influence

Figure 6 - Surface pressure coefficient on symmetry plane - influence of the differencing scheme.

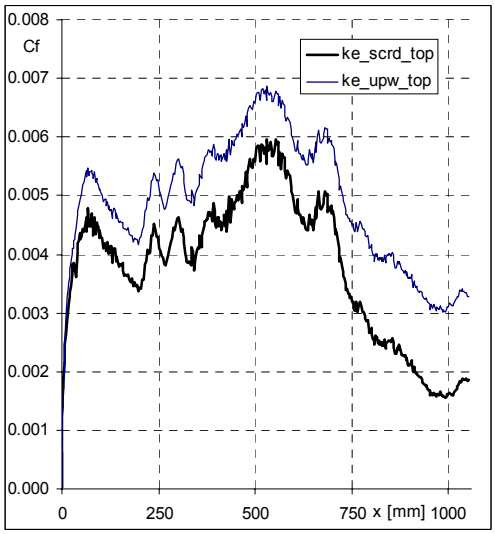

(a)

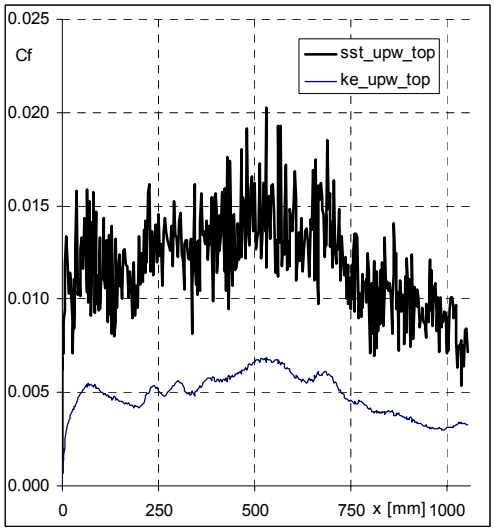

(b)

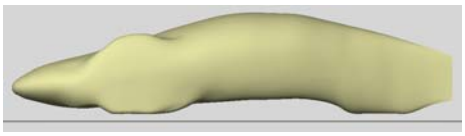

(a) - differencing scheme influence (b) - turbulence model influence

Figure 7 - Surface shear stress coefficient on symmetry plane.

Comparisons with experimental data

The comparison between the measured and the computed C_p at the car centerline is displayed in Figures 8(a) and 8(b). For these simulations, as previously referred, wind tunnel boundary conditions were taken into account. As can be seen, there is a quite good agreement between both sets of data. In the lower part of the car, pressure does not decrease as much as in the "road condition", since the flow does not accelerate as much. Comparison for the locations defined in Figure 9 is provided in the graphs of Figure 10.

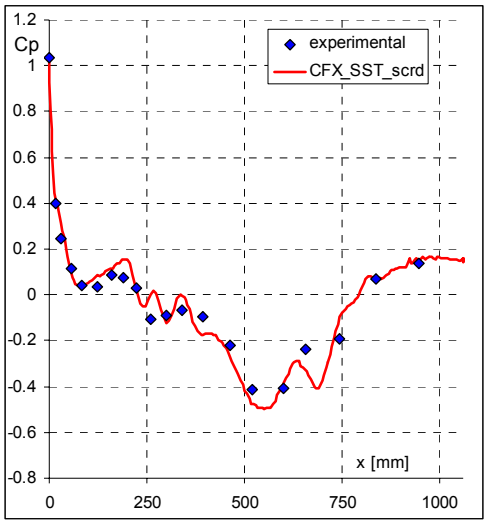

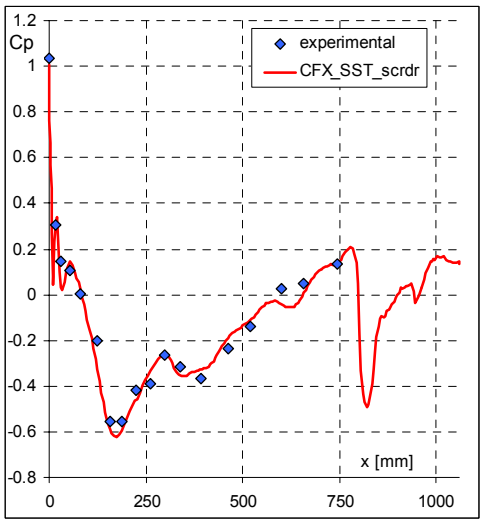

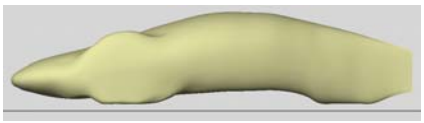

(a) - top centerline (b) - bottom centerline

Figure 8 - Surface pressure coefficient on symmetry plane: comparison between experimental and numerical results.

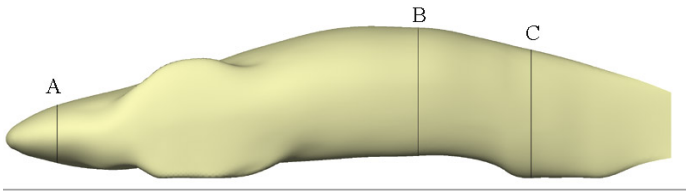

Figure 9 - Location of lines A B and C, for data in Figure 13.

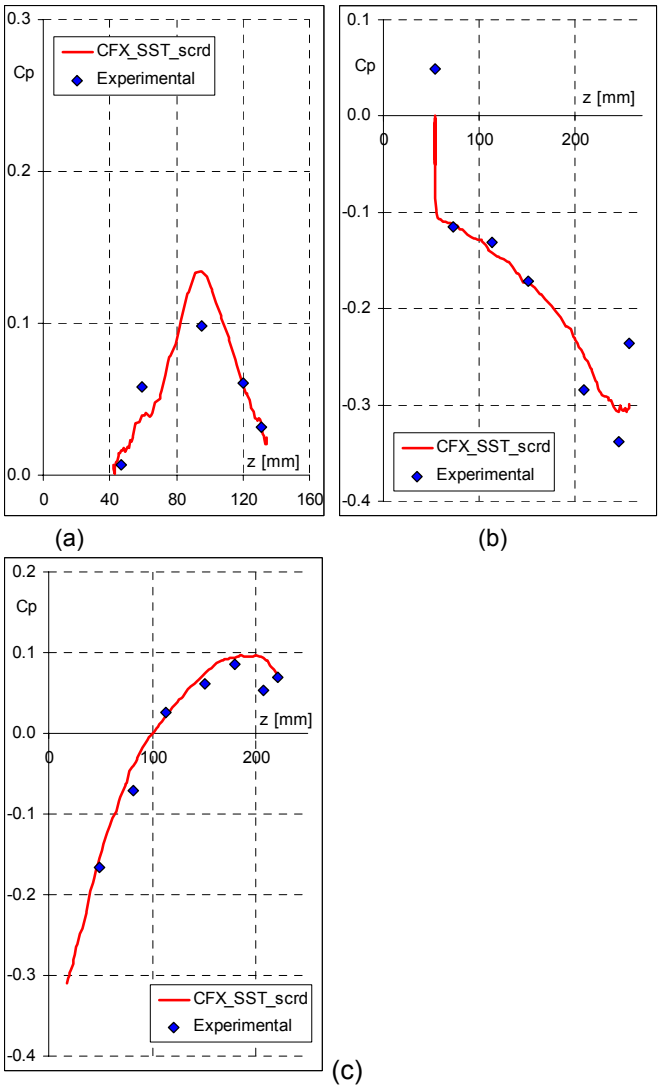

(a) - along line A (b) - along line B (c) - along line C

Figure 10 - Surface pressure coefficient along lines defined in Figure 11.

Dependence of C_D on the Reynolds number may be appreciated in Figure 11, were the measured values show the typical behaviour for a streamlined body. It is also interesting to observe the ratio between the car model drag (C_m) and the supporting wires drag (D_w), as depicted in Figure 12. At low *Re*, the wires drag represents the major portion of total drag, while with increasing *Re*, this situation is inverted.

For the simulations *Re* number of 10^6, the experimental C_D value is 0.077. The C_D coefficient predicted by the SST model, applying the correction for grid size and surface clustering, as presented previously, gives a figure of 0.0864, which represents a deviation of 10.7% from the experimental value. If one considers only the grid size influence, taking y^+=2.55 to be the best value before the exponential C_D increase as y^+ tends to 0 (cf. Figure 5b), the C_D value obtained by the Richardson extrapolation presented in Figure 5(a) is 0.0735, which represents a deviation of 4.5% of the experimental value. It should be referred that the experimental value

is probably slightly over-predicted, due to some surface roughness in the model, which is estimated to be around 40 micron.

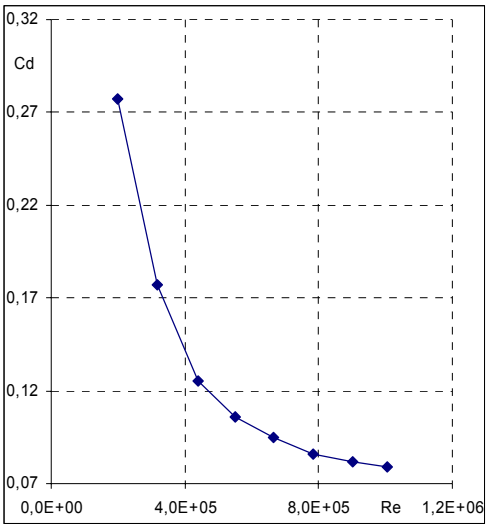

Figure 11 - Dependence of C_D with *Re* number.

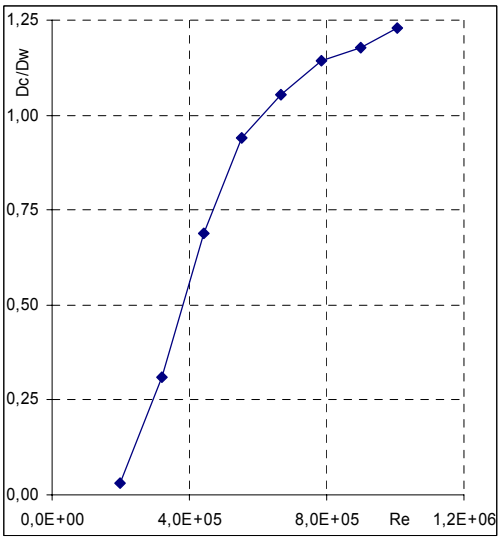

Figure 12 - Ratio between the car model drag and the wires drag.

Experimental tests were performed for non-aligned flow, at incidence angles up to 30º. Visualization with wool tufts didn't show any separation, although near the exterior wheels the flow showed some erratic behaviour, due to increased turbulence intensity. This was confirmed with numerical simulations. Figure 13 shows a top view of streamlines for this case. It is evident, in this visualization, the formation of a low intensity longitudinal vortex, thought near the car surface, no separation was detected at all.

The rolling resistance of the present car is rather low, due to the small rolling resistance coefficient for the Michelin Marathon Shell 44-406 tires, which is 1.8×10^{-3}. Considering that the total mass of the car plus the pilot is 90 kg, an approximately equal resistance force is found for aerodynamics and rolling, at 10 m/s speed. This stresses the importance of aerodynamic optimization for such vehicles, even considering that the traveling speed is relatively low.

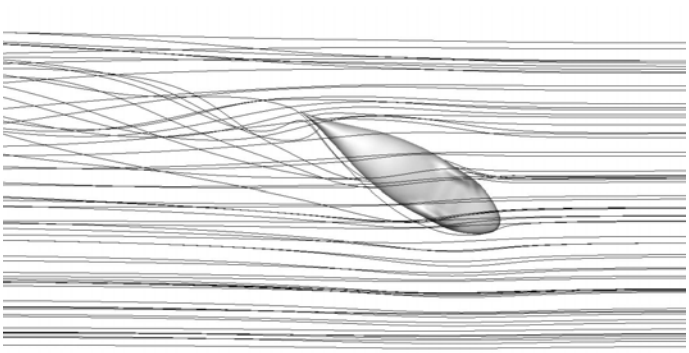

Figure 13 - Visualization of flow streamlines for a 30º incidence angle.

CONCLUSION

The present work reported on a series of numerical simulations for the airflow around a streamlined car and comparison with experimental measurements. Grid dependence tests showed that computed aerodynamic coefficients are quite sensitive to grid characteristics. The pressure component is mostly dependent on the 3D grid resolution near the car surface, while the friction component is mostly dependent on the surface y^+ value. This allows us to stress the importance of the grid surface clustering, especially for streamlined shapes, were most of the drag is due to surface friction.

The differencing scheme showed to play an important role, affecting mainly the pressure component of the drag force, with the second-order scheme providing a better agreement with the measured values, as expected. Turbulence models influenced mainly the friction component of drag. The SST model gave better C_D predictions when compared with the experimental data, although its implementation in CFX showed quite high spatial fluctuations that should be analyzed. For both models, a rather high dependence of the C_D with nodes clustering distance near the surface was found. The agreement with experimental values for CFX 5.5, using the second-order differencing scheme with the SST turbulence model is good, allowing the computation of a C_D value within 4.5% of the experimental result. Should the surface roughness of the model be lower, this agreement would be slightly better. A difference of 4% on the computed C_D value was obtained between the "road" and "wind tunnel" conditions.

In summary, turbulence modeling, differencing scheme and grid resolution are issues that play an important role on the accuracy of the predictions. Following previous

works, the present report shows that numerical tools present great potential for aerodynamic studies, especially for indicating the correct trend when comparing small changes in the shape. In fact, this report presented data obtained during the project of shape optimization for competing car. The low time needed for producing a modification and consequent testing of the results represent the major added value brought by the CFD approach.

ACKNOWLEDGMENTS

The authors whish to acknowledge their students Catarina Marques, Cristina Lourenço, Eli Abreu, Carlos Silva and Sérgio Ferreira for their work on the experimental measurements.

REFERENCES

1. Basara, B., Przulj, V. And Tibaut, P. (2001) - "On the Calculation of External Aerodynamics: Industrial Benchmarks", SAE Technical Paper Series, 2001-01-0701.
2. Han, T., Sumantran, V., Harris, C., Kuzmanov, T., Huebler, M. and Zak, T. (1996) - "Flow-Field Simulations of Three Simplified Vehicle Shapes and Comparisons with Experimental Measurements", SAE Technical Paper Series 960678.
3. Himeno, R., Takagi, M. (1990) - "Numerical Analysis of the Airflow around Automobiles Using Multi-Block Structured Grids", SAE Technical Paper Series 900319.
4. Kataoka, T., China, H., Nakagawa, K., Yanagimoto, K. and Masahiro, Y. (1991) - "Numerical Simulation of Road Vehicle Aerodynamics and Effect of Aerodynamic Devices", SAE Technical Paper Series 910597.
5. Kawaguchi, K., Hashiguchi, M., Yamasaki, R. and Kuwahara, K. (1989) - "Computational Study of the Aerodynamic Behaviour of a Three-Dimensional Car Configuration", SAE Technical Paper Series 890598.
6. Launder, B.E. and Spalding, D.B. (1974) - "The Numerical Computation of Turbulent Flows", Computer Methods in Applied Mechanics and Engineering, Vol. 3, pp. 269-289.
7. Menter, F.R. (1993) - "Multiscale Model for Turbulent Flows", 24th Fluid Dynamics Conderence, American Institute of Aeronautics and Astronautics.
8. Menter, F.R. (1994) - "Two-equation Eddy Viscosity Turbulence Models for Engineering Applications", AIAA Journal, Vol. 32, N. 8.
9. Okumura, K. and Kuriyama, T. (1995) - "Practical Aerodynamic Simulations (C_D, C_L, C_{YM}) Using a Turbulence Model and 3rd-Order Upwind Scheme", SAE Technical Paper Series 950629.
10. Ramnefors, M., Bensryd, R., Holberg, E. and Perzon, S. (1996) - "Accuracy of Drag Predictions on Cars using CFD - Effect of Grid Refinement and Turbulence Models", SAE Technical Paper Series 960681.
11. Vieser, W., Esch, T. and Menter, F. (2002) - "Heat Transfer Predictions using Advanced Two-Equation Turbulence Models", CFX Validation Report, CFX-VAL10/0602.
12. Wilcox, D.C. (1993) - "Turbulence Modeling for CFD", DCW Industries, Inc., La Canada, California, 460 p.

CONTACT

Antonio Manuel Gameiro Lopes
Departamento de Eng. Mecânica
FCTUC - Universidade de Coimbra
3030 Coimbra - Portugal
Tel: 351 239 790773
Fax: 351 239 790771
email: antonio.gameiro@dem.uc.pt
url: www.dem.uc.pt/dem/pessoas/docentes/amgl.htm